



OPEN

SUBJECT AREAS:
SILICON PHOTONICS
PHOTONIC DEVICESReceived
15 April 2014Accepted
23 July 2014Published
12 August 2014Correspondence and
requests for materials
should be addressed to
D.K. (d.knipp@jacobs-
university.de)* Current address:
Corporate Research
Department, Robert
Bosch (SEA) Pte Ltd,
Singapore.

Analyzing periodic and random textured silicon thin film solar cells by Rigorous Coupled Wave Analysis

Rahul Dewan*, Vladislav Jovanov, Saeed Hamraz & Dietmar Knipp

Research Center for Functional Materials and Nanomolecular Science, Electronic Devices and Nanophotonics Laboratory, Jacobs University Bremen, 28759 Bremen, Germany.

A simple and fast method was developed to determine the quantum efficiency and short circuit current of thin-film silicon solar cells prepared on periodically or randomly textured surfaces. The optics was studied for microcrystalline thin-film silicon solar cells with integrated periodic and random surface textures. Rigorous Coupled Wave Analysis (RCWA) was used to investigate the behaviour of the solar cells. The analysis of the periodic and random textured substrates allows for deriving optimal surface textures. Furthermore, light trapping in periodic and randomly textured substrates will be compared.

Thin-film solar cells are promising candidates for future generations of photovoltaic devices¹. In particular microcrystalline silicon ($\mu\text{c-Si:H}$) solar cells have gained considerable attention in recent years. Efficiencies higher than 10% have been demonstrated for microcrystalline silicon solar cells^{2–4}. Since the solar cell is very thin, with typical absorber thicknesses of 1–3 μm , efficient light management concepts are needed to increase the absorption of the incoming light within the solar cell. In order to determine optimal light trapping nanostructures, rigorous calculations of the optical wave propagation are required. In this study, the Rigorous Coupled Wave Analysis (RCWA) was applied to study the optics of microcrystalline silicon thin film solar cells with nanotextured interfaces. RCWA provides a fast and efficient technique in solving Maxwell's equations⁵. However, the RCWA method does not provide the electric field distribution in the individual layers of the layer stack of the solar cell. The method determines the transmission and reflection of the periodic and random surface structures for different diffraction orders. Based on the RCWA simulations, a simple model was developed that allows for determining the quantum efficiency and short circuit current based on the reflection and transmission data.

Results

Optical simulation setup and simulated device structures. A schematic diagram of the microcrystalline silicon solar cell with randomly textured interfaces is shown in Fig. 1(a). The silicon thin film solar cell consists of a randomly textured transparent conductive oxide front contact. Aluminium doped zinc oxide is a widely used transparent conductive oxide (TCO) that can be sputtered on large areas. The surface of the transparent conductive layer can be textured by wet chemical etching, so that craters are formed on the substrate⁶. As an alternative, zinc oxide and tin oxide films are prepared by Low Pressure Chemical Vapour Deposition (LPCVD) and Metal organic Vapour Deposition (MOCVD)^{7–10}. By controlling the deposition conditions the pyramidal texture of the substrate can be adjusted. Subsequently a microcrystalline p-i-n diode is prepared on the textured substrate by a Plasma Enhanced Chemical Vapor Deposition (PECVD) process. In the next step, the back contact is prepared on the solar cell. The back contact consists of a combination of a metal reflector and a thin transparent conductive oxide layer. The zinc oxide layer is introduced to reduce the parasitic plasmonic losses in the back reflector¹¹. In the case of microcrystalline silicon solar cells, the optical losses are mainly determined by nano features present at the back contact¹². In general, plasmonic losses of nanotextured metal back contacts can have a distinct effect on the quantum efficiency and short circuit current of the silicon thin film solar cells¹³.

In the following the approach to optically model the microcrystalline silicon solar cell is described. The randomly textured front contact was approximated by a triangular grating. A triangular grating, as shown in Fig. 1(b), was investigated because it resembles the randomly textured surface. The silicon solar cell structure consists of a 500 nm thick aluminium-doped zinc oxide (ZnO:Al) front contact, followed by a 1000 nm hydro-

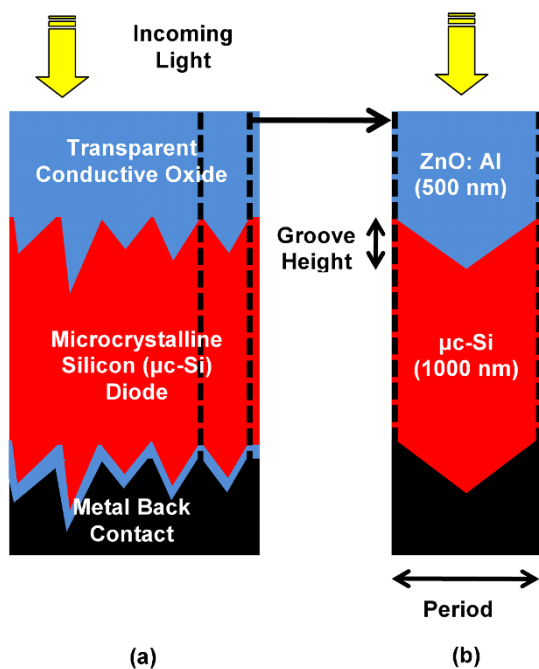


Figure 1 | (a) Schematic cross section of a microcrystalline thin-film silicon solar cell with (as-deposited) randomized textured interfaces. (b) Unit cell of the periodic arrangement used in this study, where the surface texture was approximated with a triangular grating.

generated microcrystalline p-i-n silicon diode. A perfect metal reflector (material with a high extinction coefficient) is used as back reflector. As a consequence, parasitic plasmonic losses of the metal back contact are not considered. Conformal deposition of the microcrystalline p-i-n solar cell on top of the nanotextured front contact ensures that the texturing extends all the way through the layer stack. The RCWA algorithm divides the textured solar cell in thin slices for which the transmission and reflection are calculated. However, the description of the individual slices is limited to two optical materials. Therefore, the ZnO:Al interlayer between the silicon solar cell and the back contact cannot be considered. Furthermore, the influence of the p- and the n-layer on the quantum efficiency cannot be considered. The unit cell was illuminated under normal incidence.

The real part of the refractive index and the absorption coefficient of the zinc oxide and microcrystalline silicon layers are shown in Fig. 2. Furthermore, the optical constants are included for amorphous silicon. The optical constants used for this study were obtained from optical measurements of individual layers. The optical constants were provided by Palanchoke and coworkers¹⁴. For wavelengths larger than 400 nm, the refractive indices of a-Si:H and $\mu\text{-Si}$ are comparable. The refractive index of ZnO:Al remains mostly unchanged for varying wavelengths of the incident optical spectrum. The absorption coefficient of ZnO:Al is very low which allows for high transmission into the silicon cell.

Determining the quantum efficiency and short circuit current.

The Rigorous Coupled Wave Analysis allows only for determining the transmission and reflection of different diffraction orders. The absorption of the nanotextured solar cell can be calculated by the reflection of the solar cell. However, in the case of a silicon thin-film solar cell, the parasitic absorption is largely determined by the optical losses in the front ZnO:Al layer of the p-i-n solar cell. In order to calculate the quantum efficiency of the solar cell, two separate simulations had to be performed with different optical data for the materials. In the next step, the results from the two simulations were utilized to calculate the absorption in the microcrystalline silicon layer of the solar cell. The different steps of this calculation are

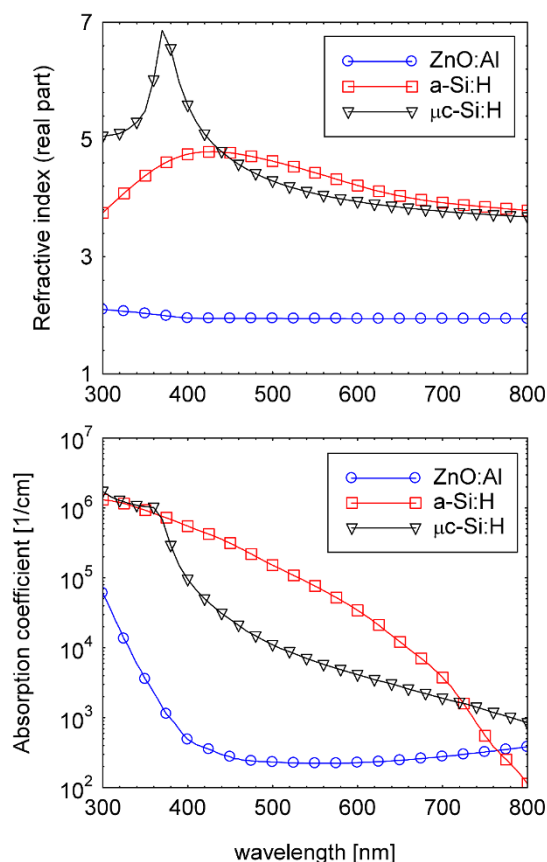


Figure 2 | Refractive index (real part) and absorption coefficient of microcrystalline silicon and aluminium doped zinc oxide. The optical data of amorphous silicon is included for comparison.

shown in Fig. 3. Along with the schematic diagrams for the setup of the simulations, the corresponding resulting curves are also shown on the right hand side of the figure. The first step involves calculating the absorption in the parasitic front layer consisting of the zinc oxide layer. By setting the extinction coefficient of an infinitely thick silicon absorber layer to zero ($\kappa_{\text{Si}} = 0$), the reflection of the layer system and the transmission through the zinc oxide layer was calculated. Using the conservation relationship of (Absorption + Transmission + Reflection = 1) for this stacked structure, we can calculate the absorption in the zinc-oxide layer

$$1 - A_{\text{Front}}(\lambda) = R_{\text{Front}}(\lambda) + T_{\text{Front}}(\lambda), \quad (1)$$

where $R_{\text{Front}}(\lambda)$ and $T_{\text{Front}}(\lambda)$ are the reflectance and transmission, respectively, of the zinc-oxide layer. In the second step, the reflection from an entire solar cell stack without any parasitic front absorption was calculated. Similar to step one, this was achieved by setting the extinction coefficient of the front stacks to zero ($\kappa_{\text{Front}} = 0$). Thus the (overestimated) absorption of the silicon absorber layer can be expressed as

$$A_{\text{Si}}(\lambda) = 1 - R_{\text{Cell}}(\lambda) \quad (2)$$

where $R_{\text{Cell}}(\lambda)$ is the total reflection of the entire solar cell stack (see Fig. 2 step 2). Subsequently, the external quantum efficiency $\text{EQE}(\lambda)$ can be calculated as

$$\text{EQE}(\lambda) \cong [R_{\text{Front}}(\lambda) + T_{\text{Front}}(\lambda)] \times [1 - R_{\text{Cell}}(\lambda)] \times \text{IQE}(\lambda), \quad (3)$$

where the absorption of the solar cell without any parasitic front absorption $A_{\text{Si}}(\lambda)$ (from Eq. 2) is corrected by the term $1 - A_{\text{Front}}(\lambda)$ (from Eq. 1). It was assumed that the internal quantum efficiency, $\text{IQE}(\lambda)$, is equal to unity, which is valid for microcrystalline silicon

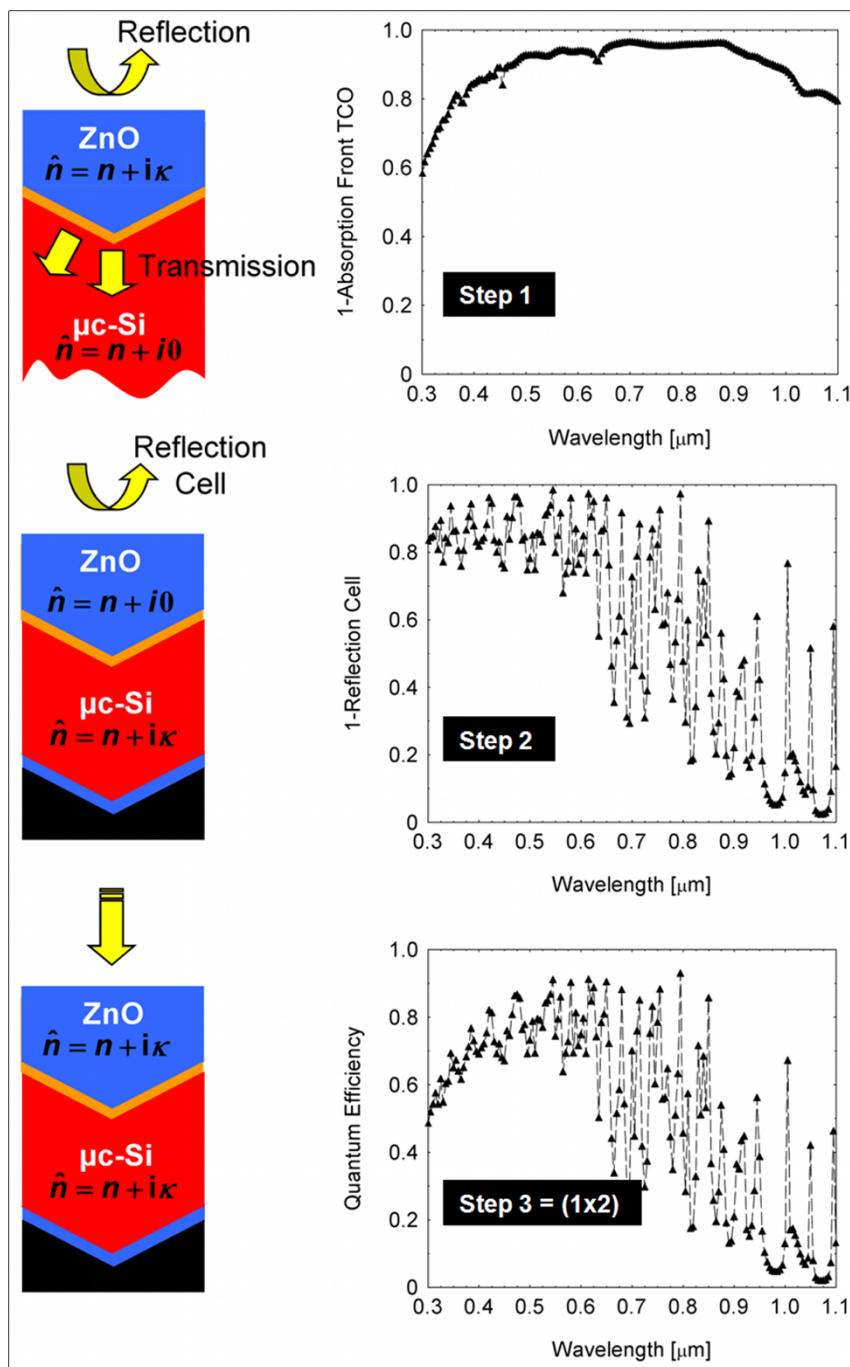


Figure 3 | Procedure for calculating the external quantum efficiency of the microcrystalline silicon solar cell. Resulting curves from each step are shown on the right hand side plots.

solar cells with absorber layers in the range of $1 \mu\text{m}^{15}$. Nevertheless, the determined quantum efficiency in Eq. 2 defines an upper limit of the achievable external quantum efficiency and short circuit current. In order to determine the open circuit voltage and fill factor of the solar cell, electrical simulations have to be carried out using the calculated generation profiles as input parameters^{16–19}.

Optimal Surface Textures of periodically textured solar cells. In the following the quantum efficiency and short circuit current was calculated for different surface textures. The thickness of the solar cell was kept constant, so that a comparison of solar cells with different surface textures is valid. The period of the interface texture was varied from 50 to 3000 nm at an interval of every 100 nm and the height of

the texture was varied in the range of 0 to 500 nm by 20 nm steps. The influence of the grating period and grating height on the short circuit current for a solar cell with a triangular grating is shown in Fig. 4(a–c). The calculated short circuit current is shown in Fig. 4(a) under blue (wavelength 300–500 nm) illumination. The short circuit current is maximized for small periods and increases with increasing height. The short circuit current is increased due to improved incoupling of shorter wavelength light. The triangular grating acts as a refractive index gradient which allows for an improved incoupling²⁰. The improved incoupling is important for shorter wavelengths, since the difference in the refractive index between the microcrystalline silicon films and the zinc oxide is largest for shorter wavelength. With increasing wavelength the difference

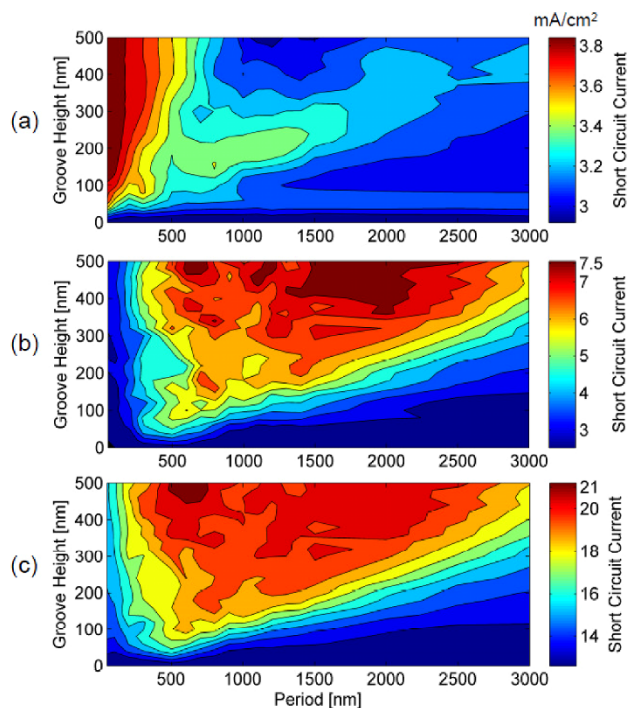


Figure 4 | Short circuit current for a 1 μm -thick microcrystalline silicon solar cell as a function of the grating period and height illuminated under (a) blue light (wavelength 300–500 nm), (b) red and infrared light (wavelength 700–1100 nm), and (c) entire sun spectrum (wavelength 300–1100 nm). The set of figures show the behaviour of solar cells with triangular grating.

decreases, and the reflection loss at the zinc oxide microcrystalline silicon interface is reduced. The improved incoupling leads to an enhancement of the short circuit by 1 mA/cm^2 up to 3.8 mA/cm^2 . The short circuit current under red and infrared (wavelength 700–1100 nm) illumination is shown in Fig. 4(b). For longer wavelengths, the short circuit current is determined by the scattering and diffraction of light at the front and back interface. The short circuit current is maximized for a period of 1500 nm. Due to scattering and diffraction the short circuit current increases from 2.5 mA/cm^2 to 7.5 mA/cm^2 . The total short circuit current of the solar cell under AM 1.5 illumination (wavelength 300–1100 nm) is given in Fig. 4(c). The total short circuit current is mainly determined by the scattering and diffraction of longer wavelengths light. The improved incoupling of light for shorter wavelengths has only a minor effect on the total short circuit current. The short circuit current is maximized for periods between 300 nm and 1000 nm.

Therefore, the optimal surface texture represents a trade-off between incoupling on one side and scattering/diffraction on the other side. For the investigated microcrystalline silicon solar cells, the maximal short circuit current reaches 21 mA/cm^2 . Compared with the short circuit current of a solar cell on a smooth substrate, the short circuit current is increased by around 60% from 13 to 21 mA/cm^2 .

Furthermore, a comparison of the calculated currents with that obtained from Finite Difference Time Domain simulations exhibits a very good agreement. Equation 3 slightly overestimated the quantum efficiency for shorter wavelengths since the absorption losses in the p-layer are ignored. The optical losses in the n-layer and the zinc oxide interlayer are rather small, so that they can be ignored. Only if nano features are introduced at the back contact, the absorption of the back reflectors significantly increases¹². Such nano features are usually introduced unintentionally due to the growth of the material.

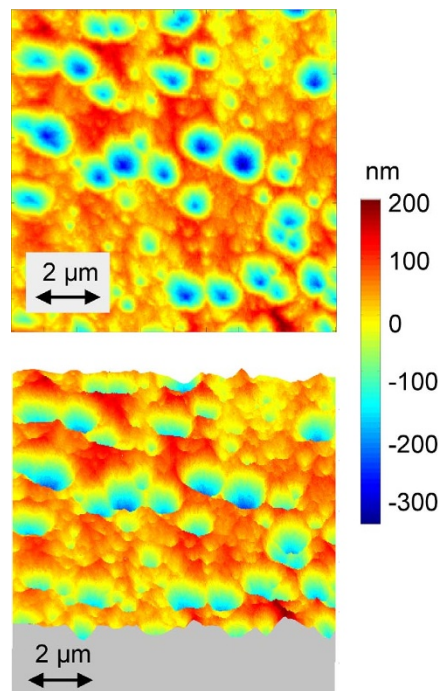


Figure 5 | Atomic force microscope scan of a nanotextured aluminium doped zinc oxide film. The film was sputtered at room temperature and subsequently etched in diluted hydrochloric acid.

The error of the presented RCWA approach was calculated to be smaller than $\pm 1.5 \text{ mA}/\text{cm}^2$.

Analyzing randomly textured substrates. Randomly textured transparent conductive oxides (TCO) are commonly used to achieve light trapping in thin film silicon solar cells. The randomly textured substrates can be realized on large areas at low cost. The randomly textured TCO can be realized by wet etching of sputtered zinc oxide (ZnO), low pressure chemical vapour deposition (LPCVD) of ZnO films or by atmospheric pressure chemical vapour deposition (APCVD) of tin oxide films [6–8]. The surface morphology ranges from crater-like features for etched ZnO to pyramid-like features for LPCVD ZnO and APCVD tin oxide. Optical measurements of the haze and angle resolved scattering properties show that the substrates exhibit very good scattering properties. In recent years significant progress has been achieved in understanding the optics in such randomly textured substrates. The scattering properties can be described successfully by scalar scattering theory^{9,10}. However, the description of the front contact of the solar cell is not sufficient to provide a fundamental understanding of optics in nanotextured solar cells. The influence of the back contact has to be considered when describing the optical properties.

In this study, we investigated aluminium doped zinc oxide layers prepared by sputtering and subsequent etching in a dilute hydrochloric (HCl) acid. Details on the preparation of the samples and the texturing process are given in Ref. 6. AFM images of a textured zinc oxide surface are shown in Fig. 5. The film was sputtered and subsequently etched in diluted hydrochloric acid (2% HCl) for 15 s. The film exhibits a root mean square roughness of 110 nm and a correlation length of 475 nm. The correlation length was determined by fitting the autocorrelation function of the AFM surface by a Gaussian distribution.

In this study, we used 1D line scans to describe the textured substrate. It allows us to study the trends in quantum efficiency and short circuit current for textured substrates of different dimensions. Following the discretization of the AFM line scans, the quantum

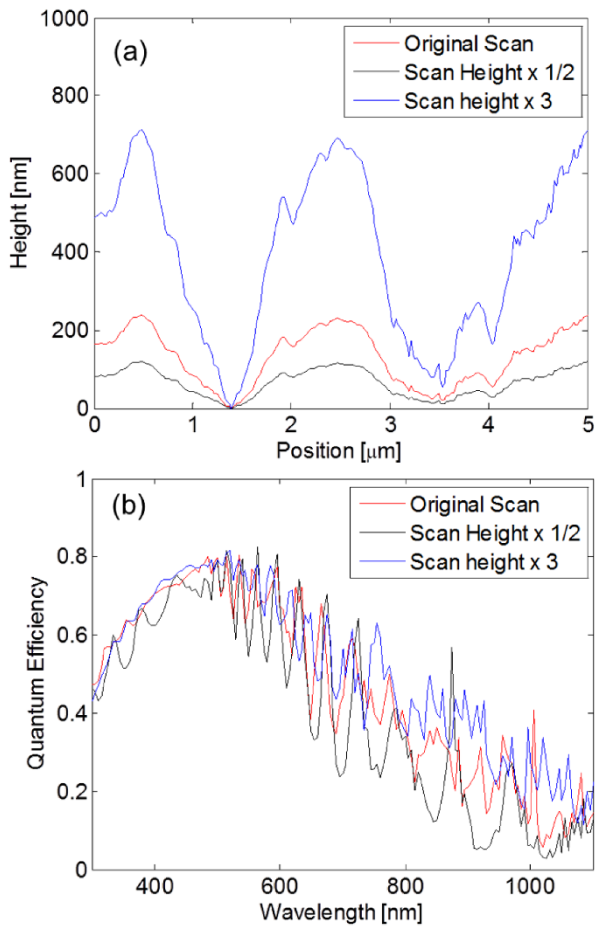


Figure 6 | (a) Line scan of a textured zinc-oxide substrate etched for 15 sec. The line profile was scaled to 50% and 300% of the original height. (b) The corresponding calculated quantum efficiency of solar cells deposited on the three different line scans shown in (a).

efficiency for solar cells deposited on the textured line scans can be calculated using Eq. 3.

The AFM line scan of a textured zinc-oxide substrate is shown in Fig. 6(a). To illustrate the effect of varying depths of the etched substrate, the line scan was scaled to different levels by multiplying the AFM scan to 50% and 300% of its original depth profile. These three generated profiles are also shown in Fig. 6(a). The corresponding calculated quantum efficiencies for solar cells deposited on the textured zinc-oxide substrates are shown in Fig. 6(b). For small heights of the surface texture, distinct interference fringes are visible. The light cannot be efficiently diffracted by the surface texture. With increasing surface texture the interference fringes start to disappear. However, they do not completely disappear since the optical simulations were carried out only for a surface scan of 5 µm. In order to compare the different scans, the short circuit current was calculated. A short circuit current of 20.2 mA/cm² was calculated for a solar cell with the original line scan. With increasing height of the surface features, the short circuit current increases while with decreasing feature size the short circuit drops. A summary of short circuit current for the different line scans is given in Table I. The total short circuit current (wavelength 300–1100 nm) and the red response of the short circuit current (wavelength 600–1100 nm) are tabulated in the table. For the line profile scaled by 500%, a gain of more than 16% in the short circuit current is calculated compared to that for the original AFM line scan. Moreover, the gain in the red response of the current highlights the light trapping effects due to surface texturing. The simulation results observed for the periodically textured surfaces

	Scaling of height level of the surface texture			Scaling of lateral length of the surface texture		
	height × 0.5	height × 1	length × 1	height × 1	height × 1	height × 1
Total Short Circuit Current [mA/cm ²]	17.60	20.20	22.30	23.50	21.50	23.60
Red short circuit current [mA/cm ²] (600–1100 nm)	8.60	10.63	12.50	13.80	11.00	13.40
				length × 1	length × 1/40	length × 1/8
				length × 1	length × 1	length × 2
				16.80	20.20	7.55

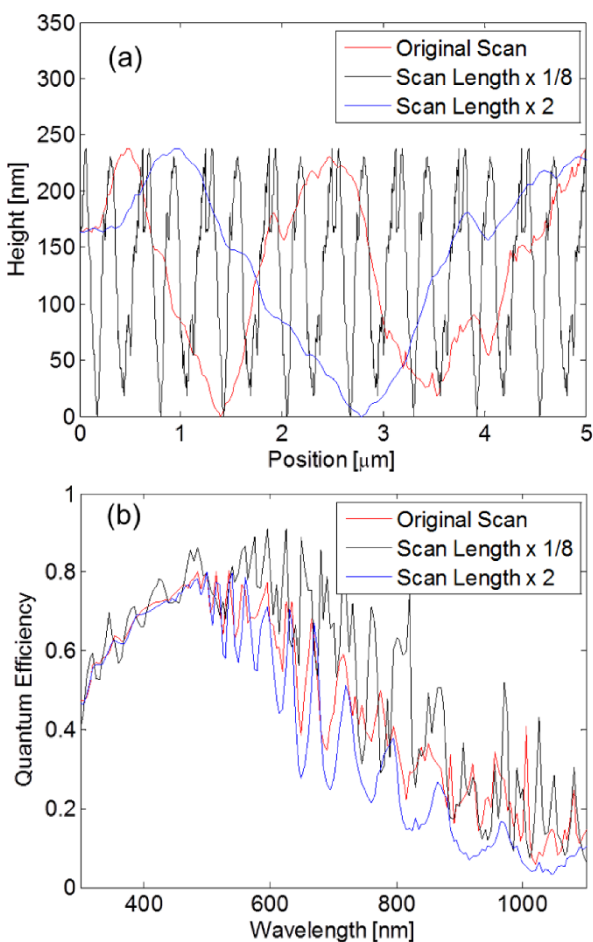


Figure 7 | (a) Line scans of three generated profiles that were varied by increasing the length span of the scan by factor 12.5% and 200%. (b) The corresponding calculated quantum efficiency of solar cells deposited on the three different line scans shown in (a).

are in good agreement with the simulations of periodically textured surfaces.

Similarly, the effect of the length span of the textured substrate was also investigated. The original line scan was scaled to factors of 12.5% and 200% in its length span. The two generated line scans and their corresponding calculated quantum efficiencies are shown in Fig. 7(a) and Fig. 7(b) respectively. By increasing the length span, the quantum efficiency of the solar cell resembles the quantum efficiency of a solar cell prepared on a smooth substrate. By shrinking the length span, the period of the features is close to 300 nm and consequently the calculated short circuit current is increased. However, when the surface features are too small (less than 100 nm) the features do not scatter longer wavelengths light efficiently, so that the quantum efficiency is reduced.

The calculated current values for solar cells on the reference line scan and the scaled scans are summarized in Table I. With increased scaling of the scans in its length, and for extremely small feature sizes, a drop in the calculated current values is observed.

Discussion

The trends observed for the randomly textured solar cell are in good agreement with the simulations of periodically textured solar cells. Furthermore, a comparison of the calculated short circuit currents for the randomly and periodically textured solar cell using comparable dimensions exhibits comparable values. The short circuit current is maximized if the period of the surface texture is in the range

between 300 nm and 1000 nm. Furthermore, the short circuit current increases with increasing height of the pyramidal texture. The short circuit current map in Fig. 4(c) shows that the short circuit current is not very sensitive to variations of the surface texture. Variations of the surface period by 100 nm do not lead to significant changes of the short circuit current. Therefore, solar cells prepared on experimentally realized randomly textured substrate exhibit high short circuit currents. The surface texture of the sputtered and subsequently etched zinc oxide substrate exhibits good dimensions for the efficient light trapping of microcrystalline silicon solar cell with a thickness of 1 μm . However, a further increase of the short circuit current can be achieved by decreasing the opening angle of the individual craters from the original values of 120–130°^{21,22}. A comparison of the simulations with other studies in literature using Rigorous Coupled Wave Analysis (RCWA), Finite Difference Time Domain (FDTD) or Finite Element Method (FEM) calculations exhibit a good agreement^{23–25}. For other material systems like amorphous silicon or different thickness of the absorber of the solar cell further investigations have to be carried out. The texture of the substrate has to be matched to the solar cell material and geometry^{26,27}. In general, it can be concluded that the optimal period increases with increasing thickness of the silicon thin film solar cell²⁷. In order to provide a more detailed simulation of the light trapping 2D scans of the substrates and the interfaces of the solar cell have to be measured by AFM or calculated by tools modeling the film growth^{28–31}. However, such calculations are computationally intensive. Nevertheless, the presented method in which the randomly texture substrates is described by a 1-dimensional scan provides a simple and very fast approach to analyze randomly textured substrates and derive optimal surface textures.

In summary, a simple and very fast method was developed to optimize the short circuit current of nanotextured thin-film solar cells. The Rigorous Coupled Wave Analysis was used to analyze the optical wave propagation in microcrystalline thin-film silicon solar cells on periodically and randomly textured substrates. RCWA facilitates a distinctly faster analysis of the optics in nanotextured thin-film solar cells compared with conventional full-wave electromagnetic simulations. The short circuit current for 1 μm thick microcrystalline silicon solar cells with surface texture is maximized if the texture period is close to 500 nm. Variations of the period of the surface texture in the range of 300 nm to 1000 nm exhibit high short circuit currents. Optical simulations for randomly textured substrates show that similar short circuit currents can be achieved for randomly textured substrates with feature is in the ranging from 300 nm to 1000 nm. The Rigorous Coupled Wave Analysis is an efficient and fast method to simulate the optics of thin film solar cells and derive optimal device dimensions.

- Konagai, M. Present Status and Future Prospects of Silicon Thin-Film Solar Cells. *Jpn. J. Appl. Phys.* **50**, 030001-1-12 (2011).
- Yamamoto, K. *et al.* Thin-film poly-Si solar cells on glass substrate fabricated at low temperature. *Appl. Phys. A* **69**, 179 (1999).
- Hänni, S. *et al.* On the Interplay between Microstructure and Interfaces in High-Efficiency Microcrystalline Silicon Solar Cells. *IEEE J. Photovoltaics* **3**, 11–16 (2013).
- Sai, H. *et al.* Microcrystalline Silicon Solar Cells with 10.5% Efficiency Realized by Improved Photon Absorption via Periodic Textures and Highly Transparent Conductive Oxide. *Appl. Phys. Express* **6**, 104101 (2013).
- Moharam, M. G. & Gaylord, T. K. Rigorous coupled-wave analysis of planar-grating diffraction. *J. Opt. Soc. Am.* **71**, 811–818 (1981).
- Berginski, M. *et al.* The effect of front ZnO surface texture and optical transparency on efficient light trapping in silicon thin-film solar cells. *J. Appl. Phys.* **101**, 074903 (2007).
- Fay, S., Kroll, U., Bucher, C., Vallat-Sauvain, E. & Shah, A. Low pressure chemical vapour deposition of ZnO layers for thin-film solar cells: temperature-induced morphological changes. *Sol. Energy Mater. Sol. Cells* **86**, 385–397 (2005).
- Hongsingthong, A., Krajangsang, T., Yunaz, I. A., Miyajima, S. & Konagai, M. ZnO Films with Very High Haze Value for Use as Front Transparent Conductive Oxide Films in Thin-Film Silicon Solar Cells. *Appl. Phys. Express* **3**, 051102-1-3 (2010).



9. Dominé, D., Haug, F.-J., Battaglia, C. & Ballif, C. Modeling of light scattering from micro- and nanotextured surfaces. *J. of Appl. Phys.* **107**, 044504 (2010).
10. Jäger, K., Fischer, M., van Swaaij, R. A. C. M. M. & Zeman, M. Designing optimized nano textures for thin-film silicon solar cells. *Optics Express*, Vol. **21**, pp.A656–A668 (2013).
11. Palanchoke, U. *et al.* Plasmonic effects in amorphous silicon thin film solar cells with metal back contacts. *Optics Express* **20**, 6340–6347 (2013).
12. Jovanov, V., Palanchoke, U., Magnus, P., Stiebig, H. & Knipp, D. Influence of back contact morphology on light trapping and plasmonic effects in microcrystalline silicon single junction and micromorph tandem solar cells. *Sol. Energy Mat. Sol. Cells* **110**, 49–57 (2013).
13. Haug, F.-J., Söderström, T., Cubero, O., Terrazoni-Daudrix, V. & Ballif, C. Plasmonic absorption in textured silver back reflectors of thin film solar cells. *J. Appl. Phys.* **104**, 064509 (2008).
14. Palanchoke, U., Magnus, P. & Stiebig, H. *private communication*.
15. Brammer, T. & Stiebig, H. Defect density and recombination lifetime in microcrystalline silicon absorbers of highly efficient thin-film solar cells determined by numerical device simulations. *J. Appl. Phys.* **94**, 1035–1042 (2003).
16. Crandall, R. S. Modeling of thin film solar cells: uniform field approximation. *J. Appl. Phys.* **54**, 7176–7186 (1983).
17. Schiff, E. A. Low-mobility solar cells: a device physics primer with application to amorphous silicon. *Sol. Energy Mat. & Solar Cells* **78**, 567–595 (2003).
18. Ding, K. *et al.* Characterization and simulation of a-Si:H/ μ c-Si:H tandem solar cells. *Sol. Energy Mat. & Solar Cells* **95**, 3318–3327 (2011).
19. Yang, K. H. & Yang, J. Y. The analysis of light trapping and internal quantum efficiency of a solar cell with grating structure. *Sol. Energy* **85**, 419–431 (2011).
20. Dewan, R. *et al.* Light trapping in thin-film silicon solar cells with submicron surface texture. *Opt. Express* **17**, 23058–23065 (2011).
21. Hüpkes, J., Owen, J. I., Pust, S. E. & Bunte, E. Chemical Etching of Zinc Oxide for Thin-Film Silicon Solar Cells. *ChemPhysChem* **13**, 66–73 (2012).
22. Dewan, R. *et al.* Analyzing nanotextured transparent conductive oxides for efficient light trapping in silicon thin film solar cells. *Appl. Phys. Lett.* **101**, 103903 (2012).
23. Rockstuhl, C. *et al.* Comparison and optimization of randomly textured surfaces in thin-film solar cells. *Optics Express*, Vol. **18**, A335–A341 (2010).
24. Fahr, S., Kirchartz, T., Rockstuhl, C. & Lederer, F. Approaching the Lambertian limit in randomly textured thin-film solar cells. *Optics Express*, Vol. **19**, A865–A874 (2011).
25. Čampa, A., Krč, J. & Topič, M. Analysis and optimisation of microcrystalline silicon solar cells with periodic sinusoidal textured interfaces by two-dimensional optical simulations. *J. Appl. Phys.* **105**, 083107 (2009).
26. Čampa, A. *et al.* Optimal design of periodic surface texture for thin-film a-Si:H solar cells. *Prog. Photovolt: Res. Appl.* **18**, 160–167 (2010).
27. Sai, H., Soto, K., Hozuki, N. & Kondo, M. Relationship between the cell thickness and the optimum period of textured back reflectors in thin-film microcrystalline silicon solar cells. *Appl. Phys. Lett.* **102**, 053509 (2013).
28. Lacombe, J., Sergeev, O., Chakanga, K., von Maydell, K. & Agert, C. Three dimensional optical modeling of amorphous silicon thin film solar cells using the finite-difference time-domain method including real randomly surface topographies. *J. of Appl. Phys.* **110**, 023102-1-6 (2011).
29. Hertel, K., Hüpkes, J. & Pflaum, C. An image processing approach to approximating interface textures of microcrystalline silicon layers grown on existing aluminum-doped zinc oxide textures. *Opt. Express* **21**, A977–A990 (2013).
30. Jovanov, V. *et al.* Influence of interface morphologies on amorphous silicon thin film solar cells prepared on randomly textured substrates. *Sol. Energy Mat. & Solar Cells* **112**, 182–189 (2013).
31. Jovanov, V. *et al.* Influence of film formation on light-trapping properties of randomly textured silicon thin-film solar cells. *Appl. Phys. Express* **7**, 082301 (2014).

Acknowledgments

The authors like to thank CIS Solartechnik and Malibu Solar for providing textured zinc oxide films. We would also like to acknowledge Malibu Solar for providing the optical constants.

Author contributions

The RCWA model and simulations of the periodic texture were done by R.D. and simulations of the random texture were performed by V.J. and S.H. D.K. supervised the project. The manuscript was prepared by R.D., V.J. and D.K. All authors discussed and analyzed the results.

Additional information

Competing financial interests: The authors declare no competing financial interests.

How to cite this article: Dewan, R., Jovanov, V., Hamraz, S. & Knipp, D. Analyzing periodic and random textured silicon thin film solar cells by Rigorous Coupled Wave Analysis. *Sci. Rep.* **4**, 6029; DOI:10.1038/srep06029 (2014).



This work is licensed under a Creative Commons Attribution-NonCommercial-NoDerivs 4.0 International License. The images or other third party material in this article are included in the article's Creative Commons license, unless indicated otherwise in the credit line; if the material is not included under the Creative Commons license, users will need to obtain permission from the license holder in order to reproduce the material. To view a copy of this license, visit <http://creativecommons.org/licenses/by-nc-nd/4.0/>